Quantitative assessment of synchronization during atrial fibrillation based on a novel index

Lin Zhang, Cuiwei Yang*, and Zhenning Nie

Abstract—**Atrial Fibrillation (AF), a chaotic rhythm classically considered with random electrical activity, is now demonstrated to show a certain degree of organization and synchronization. Rather than those traditional indices which always focus on the pairwise properties of adjacent signals, a new synchronization index-S estimator-is introduced in this paper to quantify the synchronization level for all the signals in a selected area. By evaluating a complement of the entropy of the normalized eigenvalues of the corresponding correlation matrix, S estimator is designed to be proportional to the amount of synchronization. 400 episodes of 64-channel epicardial signals acquired from four living mongrels were studied under normal sinus rhythm (SN) and AF. The results showed that there were significant decreases of S estimator for both anterior left atrium and anterior right atrium with the rhythm changing from SN to AF. After dividing the research area into eight subparts, S estimator is also capable to demonstrate the different synchronization level for each subpart and revealed the electrophysiology individual difference among four experimental subjects. In conclusion, S estimator succeeds in estimating the synchronization degree for multi-channel signals in a selected area, with no limits to the number of the signals to be analyzed. It can help us to distinguish the region with a high synchronization level during AF, which would be helpful to the clinical AF treatment and enhance our understanding of underlying mechanisms of AF.**

I. Introduction

Atrial fibrillation (AF), the most common supraventricular arrhythmia, is characterized by the chaotic contraction of atria [1]. Unfortunately, even AF is associated with such a high risk of morbidity and mortality, the causes and mechanisms of AF remains incompletely understood. Almost all cases of paroxysmal AF are caused by ectopic signals that originate in the pulmonary veins (PVs), allowing the catheter-mediated elimination of resources with clinical success rates of 70%—85% [2]. Nonetheless, according to the recent ablation therapeutic effect, even the circumferential isolation of PVs has become a standard therapy for paroxysmal AF, the endpoint is still unreached due to the high recurrence rate observed in patients, especially with persistent AF. Thus, continued efforts are underway to figure out additive strategies to improve the ablative treatment effect [3, 4]. In order to find the better ablative pathway for AF treatment, a growing number of researches and experiments are probing into the underlying mechanisms of AF.

Atrial electrical activities during AF have been discovered to represent a certain amount of organization and synchronization [5-7]. Referring to the long-standing multiple-wavelet hypothesis advanced by Moe and Abildskov [8], which proposed the fractionation of wavelets propagating through the atria results in self-perpetuating "daughter wavelets", synchronization can be explained like, when atrial regions are successively depolarized by the same and stable wavelet, the atrial electrical activity will be in a high synchronization level. Otherwise, when atrial regions are affected by multiple wavelets arising from different directions, electrical activities will represent in a low synchronization level. The measure of synchronization in atrial activation during AF may aid to study the feature of the underlying order in its activation pattern and improve our understanding of AF mechanisms. However, the traditional synchronization indices mainly focus on the analysis of two time-series signals located in the adjacent sites [6, 9-10], which is hard to represent how an atrial region is affected by the propagation of wavelets, especially during AF.

In this study a new index-S estimator-is introduced to estimate an overall synchronization degree for multiple time series. Based on the embedding technique and the measurement of contraction of embedding dimension in a state-space, S estimator helps to quantitatively assess the amount of interaction among different time series with no limits to the number of channels [11-13]. Therefore, it is suitable for the research of AF, a complex arrhythmia which shows a certain degree of synchronization in electrical activities. Considering that the four PVs are the well-accepted most frequent sources of these rapid atrial impulses, we choose to focus our attention on the analysis of the left and right atria instead of PVs.

II. METHODS

A. Data Acquisition

In this work, atrial electrograms (AEG) signals from four living mongrels (weight 13.5±2.6kg) were studied. These unipolar AEG signals were obtained by an epicardial mapping system. Two patches with total 64 electrodes were sutured onto the surface of the anterior left atrium (ALA) and anterior right atrium (ARA) (Fig.1) [14]. In addition, a separate electrode was sewn onto the apex of the left ventricle to provide a ventricular reference signal and the electrical signal

* This work was supported by the National Natural Science Foundation of China (61071004) and Science and Technology Commission of Shanghai Municipality (13441902800).

Lin Zhang is with the Department of Electronic Engineering, Fudan University, Shanghai 200433, China. (E-mail:zhanglin425@gmail.com).

*Cuiwei Yang is with the Department of Electronic Engineering, Key Laboratory of Medical Imaging Computing and Computer Assisted Intervention (MICCAI) of Shanghai, Fudan University, Shanghai 200433, China. (Corresponding author, phone & fax: +8621-65643709; e-mail: yangcw@fudan.edu.cn).

Zhenning Nie is with Department of Cardiology, Zhongshan Hospital, Fudan University, Shanghai Institute of Cardiovascular Diseases, Shanghai 200032, China (e-mail: nie.zhenning@zs-hospital.sh.cn).

978-1-4244-7929-0/14/$26.00 ©2014 IEEE

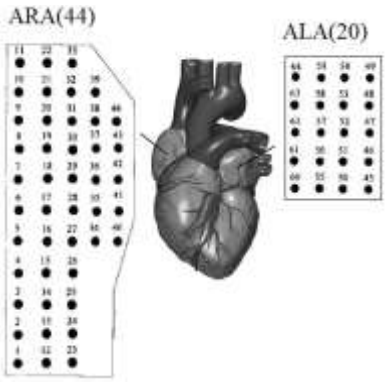

Fig.1. Schematic of atrial epicardial mapping position. Two flexible patches were positioned on Anterior Left Atrium (ALA), Anterior Right Atrium (ARA). The number in the parentheses indicates the amount of electrodes on each patch. The unipolar electrodes had the horizontal and vertical spacing as follows: 3.5 mm, 3.5mm.

of the aortic root was acquired as an electrical reference ground. All the electrodes were connected to the FDEMS-2 epicardial mapping system that was developed by Fudan University, Shanghai, China [15]. All the signals were amplified with isolated amplifier with adjustable gain (25-2000), filtered with the fixed bandwidth (3.5-600 Hz), and digitized to a 2 kHz sampling rate at 16-bit resolution.

The experiment was processed based on the cholinergic AF model. AF was induced by a burst-pacing stimulus at frequency of 20 Hz, pulse width of 2ms, and duration of 5s. The stimulus was transmitted to the pairs of stimulating electrodes placed on the right atrial appendage and the interface between the superior vena cava and the right atrium [14, 15]. We had recorded sinus AEG signals before stimulus and the AEG signals with AF duration more than 3 minutes. Prior to the processing, the AEG signals were segmented into episodes with data length of 20s (40000 points), which is believed to contain sufficient atrial activation information for synchronization analysis.

B. Signal Preprocessing

To remove ventricular artifact on the AEG signals, a least mean square (LMS) adaptive filter based on the model of noise-canceller was applied [16]. The reference signal of noise was the ventricular signal collected from the apex of the left ventricle and the contaminated signal was original AEG signal which contained the undesirable ventricular signal. By adaptive filter self-adjusting to the optimal filter weights, the optimal estimate of noise (ventricular signal) was worked out. After eliminating the ventricular signal for all the 64-channlel AEG signals, the expected AEG signals were acquired.

C. S estimators

S estimator is a measure quantifying the amount of interaction among different time series [12, 13]. It is a function of the normalized eigenvalues of a cross correlation matrix constructed from generic multivariate time series [13]. In this paper, we adopt S estimator to evaluate the synchronization degree of the AEG signals obtained from the ALA and ARA during different rhythms, where synchronization is defined as a result of how multiple subsystems (myocardia) are affected by the common or multiple external forcing. When we estimate one S estimator value for each patch, the number of AEG signals to be calculated depends on the quantity of electrodes positioned on the patch. Briefly, S estimator can be acquired as follows [11-13, 17]:

(1) Prepare the corresponding cross correlation matrix C of size $N\times N$ for each patch (N electrodes positioned on the patch).

(2) Calculate all the eigenvalues of the correlation matrix C, i.e., $\lambda_i, i=1,...N$, based on the Principal Components Analysis (PCA).

(3) Compute an entropy quantity E after normalizing the corresponding eigenvalues $\lambda_i^{'}=\frac{\lambda_i}{trace(C)}=\frac{\lambda_i}{N}$,

$$E=-\sum_{i=1}^{N}\lambda_i^{'}\log\lambda_i^{'} \qquad (1)$$

Obviously, the entropy quantity E is proportional to the embedding dimension of those multiple time series, thus inversely proportional to the degree of synchronization.

(4) Propose S estimator to evaluate the degree of synchronization with the value of entropy E:

$$S=1-\frac{E}{\log(N)} \qquad (2)$$

According to the multiple wavelets hypothesis [8], S estimator that can be used to estimate the degree of synchronization is based on the rationale that, if an unstable wavelet or many different wavelets are propagating through atrial regions, the synchronization degree of those multiple AEG signals will be low and the morphology of those multiple signals will show up as significant differences. Those differences in morphology will lead to a large embedding dimensionality of the state-space and result in a high dispersion of eigenspectrum of the corresponding cross correlation matrix, which could be explained as there are more significant components. Therefore, the entropy quantity will be large and the value of S estimator will be accordingly low (S=0 is the extreme example of low synchronization level, which means all the AEG signals are generated totally independent, and the atrial region is affected by numerous disorganized wavelets simultaneously). On the contrary, S estimator will be a high value when a stable wavelet propagating through the atrial region during SN or atrial tachycardia, which indicates a high synchronization level of electrical activities.

III. RESULTS

A. Assessment of Synchronization on ALA and ARA during Different Rhythms

Taking a global view to analyze the synchronization level for different atrial parts, each patch (ALA and ARA) was regarded as a whole to be estimated for a value of S estimator. We randomly selected 100 episodes of AEG signals under SN and AF for each mongrel. The representative data bars in Fig.2 exhibited S estimators of multi-channel epicardial signals acquired from four mongrels. With the cardiac rhythm changing from SN to AF, the result indicated the S estimators decreased significantly ($p<0.001$, Wilcoxon–Mann–Whitney

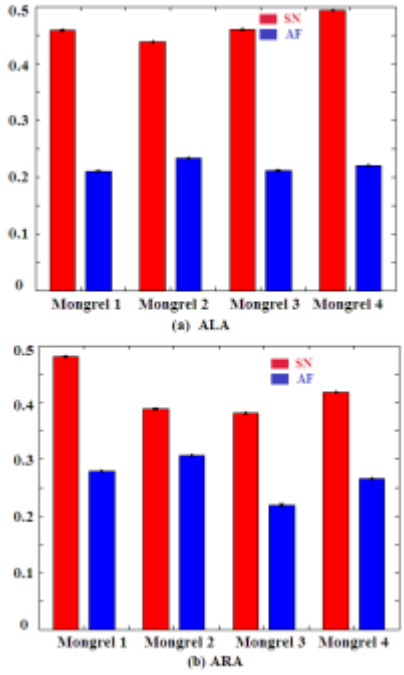

Fig.2 Spatial distribution of synchronization of ALA (a) and ARA (b) during SN and AF. White bars on the left presented average degrees and standard deviations (whiskers) of synchronization degrees during SN, and black bars on the right showed the average degrees of synchronization during AF. The S estimators of both ALA and ARA decreased significantly ($p < 0.001$, Wilcoxon–Mann–Whitney test) from SN to AF.

test) for all the mongrels, both on ALA and ARA. The atrial electrical activities were demonstrated to change into disorganized and less synchronized during the fibrillatory rhythm.

B. Assessment of Synchronization on subparts during Different Rhythms

In order to figure out a more specific region of interest, we divided the original research area into eight subparts, with each subpart of ALA and ARA respectively contained five electrodes and eleven electrodes, as shown in Fig.3. The S estimator value for eight subparts during SN and AF were represented in Fig.4. On one hand, the individual difference was strengthened when assessing the synchronization degree for subdivided atrial parts under both rhythms. On the other hand, as might be expected, all the subpart S estimators decreased dramatically when the cardiac rhythm changed from SN to AF. However, there were still some regions remaining at a high synchronization level (S estimator is large) during AF (such as the R1 on the ARA for four mongrels).

IV. Discussion

As it shown in Fig.2, S estimators for four mongrels slightly vary from one individual to another. However, the data reveal that all the ALA and ARA S estimators are far from the expected high synchronization degree (S=1) during SN, even the wavelet propagates through ALA and ARA is generated by sinoatrial node (SAN), which should be stable and continuous. Besides taking the quality of experiment

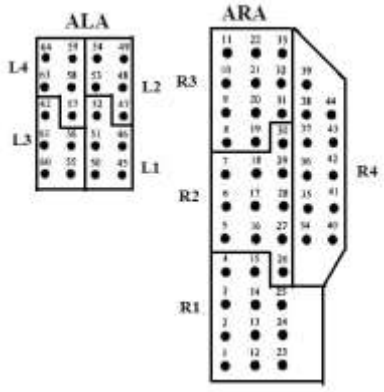

Fig.3 Schematic of the divided patches of ALA and ARA. The divided patch on the left (ALA) included four subparts and each subpart had five unipolar electrodes. And the divided patch on the right side (ARA) included four subparts and each subpart had eleven unipolar electrodes.

environment into account, we have to recognize that AEG acquired from an electrode is the integrated potential of multiple myocardial cells when we estimate the synchronization based on the signal morphology. The morphology of the integrated AEG will be affected by the position and contact degree of the electrodes on the surface of atria. Meanwhile, the signal morphology depends on the tissue anisotropy, curvature of wavefront and different transmural velocity [18]. Those might be the factors which make the synchronization degrees for ALA and ARA are not as high as expected during SN. Nonetheless, we can still find out all the S estimator values decrease significantly when the cardiac rhythm changes from SN to AF. It demonstrates electrical activities on ALA and ARA are turning into asynchronous and disorganized during AF, indicating there exist some external forcing other than SAN.

In order to get more detailed information about the electrical activities of ALA and ARA, we calculate the subpart S estimators of eight divided regions. According to inter-individual variability shown in Fig.4, difference in heart size and electrophysiological characteristics of each subject may enlarge the distinction of the value of S estimator. However, with all the subpart S estimators decrease during AF, the subpart R1 seems to maintain a high synchronization degree for all mongrels. The result is consistent with the definition of synchronization caused by the external forcing, because R1 is the region close to the stimulus position among the research area. Nevertheless, even R1 subpart keep in a high synchronization level, more subjects or the clinical data should be further verified to find out the region which is responsible for AF maintenance and help to advance the new strategies for AF treatment [19].

The distribution of Shannon entropy based on the cross correlation is shown in Fig.5, where the cross correlation value is calculated between two adjacent signals and the Shannon entropy is calculated by the variation of pairwise cross-correlation. Rather than the bi-channel synchronization distribution, which may indicate too many regions of interest to decentralize our attention from the real crucial abnormal region, S estimator makes it possible to help us focus our attention to ectopic area gradually from the large region to a small part.

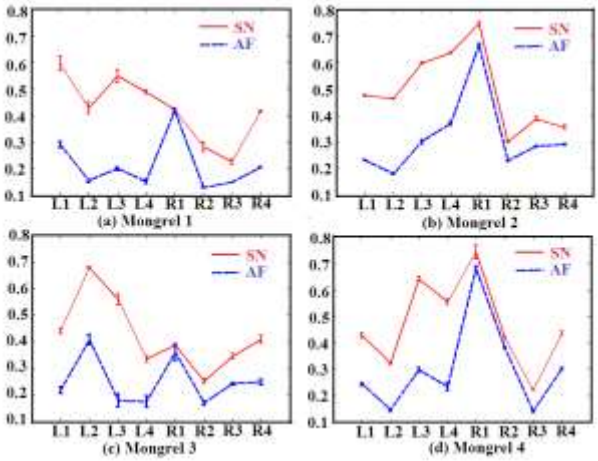

Fig.4 Subpart spatial distribution of synchronization of ALA and ARA for four mongrels during SN and AF. The full lines with error bars (standard deviations) represented the value of S estimator for eight subparts during SN; the dotted lines with error bars (standard deviations) represented the value of S estimator for eight subparts during AF.

V. Conclusion

In this work we introduced S estimator to quantify the synchronization of multi-channel AEG signals. It demonstrates the synchronization level on different atrial parts. Even during AF, this synchronization index would indicate the area with a high synchronization degree. Because the number of channels chosen to be calculated is not restricted, S estimator can help to estimate the synchronization degree for any atrial part in any size. It probably helps us to recognize the abnormal region from a large scale to the small one, which would make the contribution to improve the AF treatment effect.

References

[1] R. De Caterina, D. Atar, S. H. Hohnloser, and G. Hindricks, "2012 focused update of the ESC Guidelines for the management of atrial fibrillation," *European Heart Journal*, vol. 33, pp. 2719–2747, 2012.

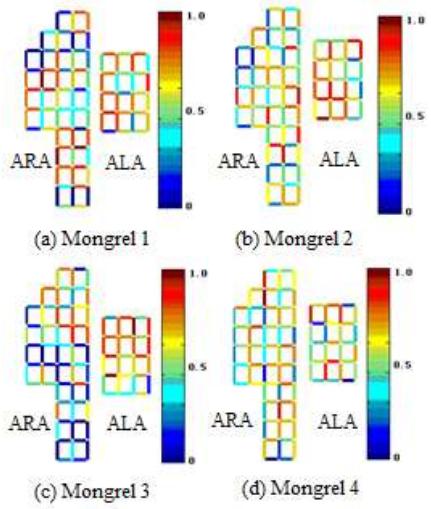

Fig.5 Distribution of Shannon entropy based on the cross-correlation value of adjacent signals acquired from ALA and ARA. All the cross-correlation values are normalized by dividing the maximum cross-correlation value.

[2] H. Calkins, M. R. Reynolds, P. Spector, M. Sondhi, Y. Xu, A. Martin, C. J. Williams, and I. Sledge, "Treatment of Atrial Fibrillation With Antiarrhythmic Drugs or Radiofrequency Ablation Two Systematic Literature Reviews and Meta-Analyses," *Circulation: Arrhythmia and Electrophysiology*, vol. 2, no. 4, pp. 349–361, 2009.

[3] S. Ernst, F. Ouyang, F. Löber, M. Antz, and K. H. Kuck, "Catheter-induced linear lesions in the left atrium in patients with atrial fibrillation An electroanatomic study," *Journal of the American College of Cardiology*, vol. 42, no. 7, pp. 1271–1282, 2003.

[4] P. Jaïs, M. Hocini, L. F. Hsu, P. Sanders, C. Scavee, R. Weerasooriya, L. Macle, F. Raybaud, S. Garrigue, D. C. Shah, P. L. Metayer, J. Clémenty, M. Haïssaguerre, "Technique and results of linear ablation at the mitral isthmus," *Circulation*, vol. 110, no. 19, pp. 2996–3002, 2004.

[5] G. W. Botteron, J. M. Smith, "A technique for measurement of the extent of spatial organization of atrial activation during atrial fibrillation in the intact human heart," *IEEE Transactions on Biomedical Engineering*, vol. 42, no. 6, pp. 579–586, 1995.

[6] M. Masè, L. Faes, R. Antolini, M. Scaglione, F. Ravelli, "Quantification of synchronization during atrial fibrillation by Shannon entropy: validation in patients and computer model of atrial arrhythmias," *Physiological measurement*, vol. 26, no. 6, pp. 911, 2005.

[7] U. Richter, L. Faes, A. Cristoforetti, M. Masè, F. Ravelli, M. Stridh, L. Sörnmo, "A novel approach to propagation pattern analysis in intracardiac atrial fibrillation signals," *Annals of biomedical engineering,* vol. 39, no. 1, pp. 310-323, 2011.

[8] G. K. Moe, J. A. Abildskov, "Atrial fibrillation as a self-sustaining arrhythmia independent of focal discharge," *American heart journal* , vol. 58, no. 1, pp. 59–70, 1959.

[9] L. Faes, G. Nollo, R. Antolini, F. Gaita, F. Ravelli, "A method for quantifying atrial fibrillation organization based on wave-morphology similarity," *IEEE Transactions on Biomedical Engineering*, vol. 49, no. 12, pp. 1504-1513, 2002.

[10] A. Buttu, S. Volorio, A. Forclaz, P. Pascale, S. M. Narayan, E. Pruvot, J. M. Vesin, "Tracking of stepwise ablation of persistent atrial fibrillation using synchronization of nearby electrogams," *In: IEEE computing in cardiology conference*, pp. 505-508, 2011.

[11] C. Carmeli, M. G. Knyazeva, G. M. Innocenti, O. D. Feo, "Assessment of EEG synchronization based on state-space analysis," *Neuroimage* vol. 25, no. 2, pp. 339–354, 2005.

[12] S. Boccaletti, J. Kurths, G. Osipov, D. L. Valladaresb, C.S. Zhou, "The synchronization of chaotic systems," *Physics Reports,* vol. 366, no. 1, pp. 1–101, 2002.

[13] D. M. Walker, C. Carmeli, F. J. Pérez-Barbería, M. Small, E. Pérez-Fernández, "Inferring networks from multivariate symbolic time series to unravel behavioural interactions among animals," *Animal Behaviour*, vol. 79, no. 2, pp.351–359, 2010.

[14] Y. Chen, Z. Wu, C. W. Yang, J. Shao, K. L. K. Wong, D. Abbott, "Investigation of atrial vulnerability by analysis of the sinus node EG from atrial fibrillation models using a phase synchronization method," *IEEE Transactions on Biomedical Engineering,* vol. 59, no. 9, pp. 2668–2676, 2012.

[15] W. J. Lu, C. W. Yang, Z. X. Fang, X. P. Liu, X. Zhu, "Implementation of a novel interpolating method to epicardial potential mapping for atrial fibrillation study," *Computers in Biology and Medicine,* vol. 40, no.4, pp. 456–463, 2010.

[16] L. Q. Sun, L. Liu, Y. L. Wang, C. W. Yang, "An Adaptive Filtering Algorithm applied to Inhibit the Interference from the Ventricular during Atrial Epicardial Mapping Experiment(Translation Journals style)," *Chinese Journal of Medical Instrumentation*, vol. 35, no. 4, pp. 243–245, 2011.

[17] C. Carmeli, "Assessing cooperative behavior in dynamical networks with applications to brain data". *Lausanne: Ecole Polytechnique Federal de Lausanne*, 2006.

[18] R. P. Houben, N. de Groot, J. L. Smeets, A. E. Becker, F. W. Lindemans, M. A. Allessie, "S-wave predominance of epicardial electrograms during atrial fibrillation in humans: indirect evidence for a role of the thin subepicardial layer," *Heart Rhythm*, vol. 1, no. 6, pp. 639-647, 2004.

[19] F. Ravelli, M. Masè, A. Cristoforetti, M. Del Greco, M. Centonze, M. Marini, M. Disertori, "Anatomic Localization of Rapid Repetitive Sources in Persistent Atrial FibrillationFusion of Biatrial CT Images With Wave Similarity/Cycle Length Maps," *JACC: Cardiovascular Imaging*, vol. 5, no. 12, 2012.